

A Cuboctahedral Supramolecular Capsule by 4:4 Self-Assembly of Tris(Zn^{II}-cyclen) and Trianionic Trithiocyanurate in Aqueous Solution at Neutral pH (Cyclen = 1,4,7,10-Tetraazacyclododecane)

Shin Aoki,^[a] Motoo Shiro,^[b] and Eiichi Kimura*^[a]

Abstract: A 1:1 mixture of a tris(Zn^{II}-cyclen) (**1**: [Zn₃L¹], L¹ = 1,3,5-tris-(1,4,7,10-tetraazacyclododecan-1-ylmethyl)benzene) and trithiocyanuric acid (TCA) yielded a 4:4 self-assembly complex [(Zn₃L¹)₄(TCA³⁻)₄] (**6**) through the formation of Zn^{II}-S⁻ coordination bonds and hydrogen bonds between 1,3,5-triazine N and cyclen NH (cyclen = 1,4,7,10-tetraazacyclododecane); the supramolecular capsule structure was revealed by X-ray crystal structure analysis. The capsule exterior represents a twisted cuboctahedral framework containing a nanoscale truncated tetrahedral cavity. The crystal data: formula C₁₄₄H₃₀₈N₇₂O₅₈S₁₂Zn₁₂ (**6**[NO₃]₁₂·22H₂O), M_r = 5145.75, cubic, space group F432 (No. 209), a = 39.182(1) Å, V = 60153(3) Å³, Z = 8, R = 0.100, R_w = 0.259. Lipophilic organic molecules with the matching sizes, for example, ([D₄]-2,2,3,3)-3-(trimethylsilyl)propionic acid (TSP), 1-adamantanecarboxylic acid, 2,4-dinitrophenol (2,4-DNP), adaman-

tane (ADM), or the tetra-*n*-propylammonium (TPA) cation, are encapsulated in the inner cavity, as revealed by remarkable upfield shifts of the ¹H NMR signals of these guest molecules. The encapsulation of ADM was confirmed by X-ray crystal structure analysis. Crystal data of the ADM-encapsulating complex: formula C₁₅₄H₃₃₄N₇₂O₆₃S₁₂Zn₁₂ (**6**-ADM[NO₃]₁₂·27H₂O), M_r = 5372.06, cubic, space group F432 (No. 209), a = 39.061(1) Å, V = 59599(3) Å³, Z = 8, R = 0.103, R_w = 0.263. The 4:4 self-assembly was stabilized by incorporation of one of these guest molecules. The apparent 4:4 self-assembly constants for **6** in the presence of an excess amount of a guest TPA, log K_{app} (K_{app} = [6-TPA]/

[1]⁴[TCA]⁴) (M⁻⁷), were determined to be 34.0 ± 2.0 and 35.5 ± 3.0 by potentiometric pH and UV spectrophotometric titrations, respectively. An apparent encapsulation constant for 2,4-DNP, log K_{enc} (K_{enc} = [6-2,4-DNP]/[6][2,4-DNP]) (M⁻¹), was 6.0 ± 0.1 at pH 7.0 (50 mM HEPES with I = 0.1 (NaNO₃)), as determined by UV titrations. The lipophilicity of the inner cavity was close to that of 2-propanol, as a quantum yield (Φ) of 0.24 ± 0.1 for the fluorescent emission of 7-diethylaminocoumarin-1-carboxylic acid (20 μM) in the capsule was close to the Φ of 0.22 found for 2-propanol. Encapsulation properties of the present Zn^{II}-containing cage have been compared with those of cyclodextrins and Fujita's Pd^{II}-containing supramolecular cage. The exterior chirality of the 4:4 complex was controlled from within by an encapsulated chiral guest molecule, 2,10-camphorsultam, as indicated by Cotton effects in the circular dichroism spectra.

Keywords: host-guest systems · molecular recognition · nanostructures · supramolecular chemistry · zinc

Introduction

Supramolecular architectures formed by artificial self-assembly of small molecules under equilibrium conditions have

[a] Prof. E. Kimura, Dr. S. Aoki
Department of Medicinal Chemistry
Faculty of Medicine, Hiroshima University
Kasumi 1-2-3, Minami-ku, Hiroshima, 734-8551 (Japan)
Fax: (+81)82-257-5324
E-mail: ekimura@hiroshima-u.ac.jp

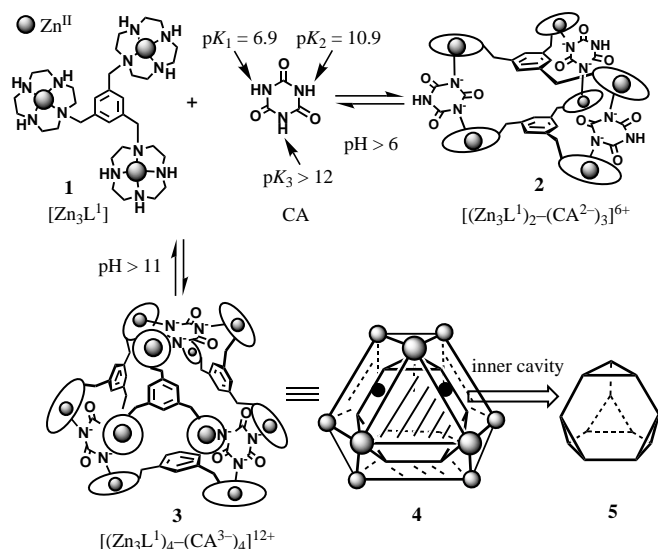
[b] Dr. M. Shiro
Rigaku Corporation X-ray Research Laboratory
Matsubaracho 3-9-12, Akishima, Tokyo, 196-8666 (Japan)

Supporting information for this article is available on the WWW under <http://www.wiley-vch.de/home/chemistry/or> from the author. Procedures for isolation of **6**-3-NP, **6**-(4-NP)⁻, **6**-(2,4-DNP)⁻, and **6**-((1*S*,2*R*,4*R*)-CST) complexes; and ¹H spectra (aromatic region) of **6**-guest complexes; ESI-MS spectra of **6**-3-NP and **6**-((1*S*,2*R*,4*R*)-CST).

great potential for selective guest inclusion, involving molecular recognition, or for new organic reaction sites.^[1] While supramolecular chemistry in aprotic media is common and well developed, self-assembly in aqueous solution is not so extensively exploited except for a few cases in which metal-ligand coordination bonds are exploited.^[2-4] Furthermore, quantitative evaluations of supramolecular complexation and recognition mechanisms, particularly in aqueous solution, have been almost nonexistent.

We have found that bonding between imide anions and the fifth coordination sites of Zn^{II}-cyclen complexes (cyclen = macrocyclic tetraamine 1,4,7,10-tetraazacyclododecane) is a new effective method to construct reversible and yet stable supramolecular complexes in aqueous solution.^[5-7] Very recently, we observed that a trimeric Zn^{II}-cyclen complex linked with a 1,3,5-trimethylbenzene spacer (**1**: [Zn₃L¹], L¹ =

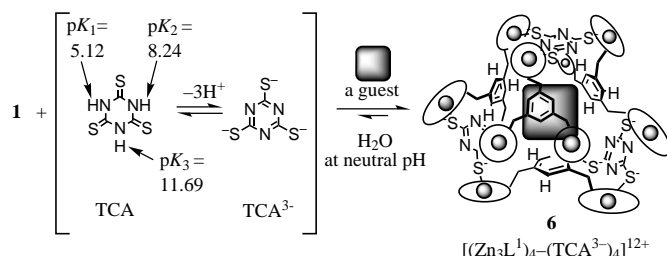
1,3,5-tris(1,4,7,10-tetraazacyclododecan-1-ylmethyl)benzene^[8] quantitatively bound cyanuric acid (CA) to form a 2:3 sandwich-like supramolecular complex (**2**: $[(Zn_3L^1)_2-(CA^{2-})_3]$) at neutral pH and a 4:4 cage complex (**3**: $[(Zn_3L^1)_4-(CA^{3-})_4]$) at basic pH, as determined by X-ray crystallography (Scheme 1).^[7] The potentiometric pH titration supported the deprotonation of the two NHs from CA and stability of the resulting complex **2** with its speciation of



Scheme 1.

>98%, when **1** (=1.0 mM) and CA (=1.5 mM) were mixed aqueous solution at pH 6. At higher pH (>11), further deprotonation from the third imide NH apparently occurred to yield the novel 4:4 supramolecular complex **3**. The exterior framework of **3** can be schematically represented as a cuboctahedron **4**, which is composed of two types of triangles, tetrahedrally facing, linked together through four rectangular spaces with the twelve Zn^{II} locating at twelve vertices. Inside is a hollow, which can be visualized as a highly symmetrical truncated tetrahedron **5** and was thought to offer a good guest inclusion site. However, it was found that the isolated **3** collapsed into **2** and **1** in aqueous solution at neutral pH.

For construction of a more robust supramolecular cage in practical conditions, we now have replaced CA with trithiocyanuric acid (TCA) (Scheme 2). A possible advantage of



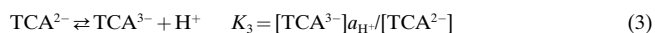
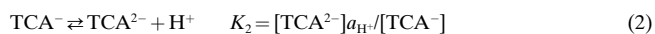
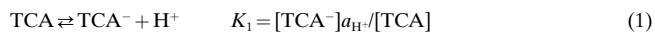
Scheme 2.

TCA over CA is that its three deprotonation constants (pK_a) are lower than those for CA, so that the anionic TCA^{3-}

species could be attained at lower pH.^[9] Another advantage would be that once formed TCA^{3-} tends to aromatize to a 1,3,5-triazine structure and the anions localize on the exocyclic sulfur atoms; this permits strong $Zn^{II}-S^-$ interactions.^[10] Herein we present a new and interesting supramolecular capsule **6** formed by self-assembly of four molecules each of **1** and TCA^{3-} reversibly encapsulating a variety of hydrophobic and cavity-size-matched guest molecules in neutral aqueous solution.^[11]

Results and Discussion

Deprotonation constants of trithiocyanuric acid (TCA): The three deprotonation constants of TCA at 25 °C and $I = 0.1$ ($NaNO_3$), defined by Equations (1)–(3), were determined to be 5.12 ± 0.05 (pK_1), 8.24 ± 0.05 (pK_2), and 11.69 ± 0.05 (pK_3) by our potentiometric pH titrations under the reaction conditions for the following supramolecular complexation.^[9] These values are lower than those found for CA ($pK_1 = 6.85$, $pK_2 = 10.91$, and $pK_3 > 12$).^[7]



Isolation and structure of the 4:4 supramolecular cage **6**:

Slow evaporation of a solution of $1[NO_3]_6 \cdot H_2O \cdot 0.5 EtOH$,^[8] TCA, and $NaNO_3$ in aqueous solution (pH 8.0 adjusted by $NaOH$) yielded fine colorless prisms. The elemental analysis was consistent with a 1:1 stoichiometry of **1** and TCA^{3-} with $3NO_3^-$ counteranions.

The 4:4 complex structure **6** was determined by X-ray crystal structure analysis. The crystal data are summarized in the Experimental Section. Figures 1a and b are space-filling drawings of **6** viewed along the C_3 and C_2 symmetry axes, respectively. Four molecules of **1** are displayed in light green, green, light blue, and blue. The 1,3,5-triazine rings of TCA^{3-} are orange with yellow exocyclic sulfur anions. The exterior diameter of **6** is 2.4–2.5 nm. The coordination mode around TCA^{3-} is shown in Figures 1c and d. Each triangular TCA^{3-} links to three Zn^{II} -cyclen moieties through $Zn^{II}-S^-$ coordination bonds (average length is 2.3 Å) and $N \cdots H-N$ hydrogen bonds (average length between two nitrogens is 2.9 Å). Since the three C-S- Zn^{II} bonds around all of the four TCA^{3-} units in **6** are bent by 100° in a clockwise fashion or in a counterclockwise fashion, **6** is a chiral supermolecule. The red dot in Figure 1d indicates one of the C_3 axes perpendicular to the center of 1,3,5-triazine ring of TCA^{3-} unit; this axis coincides with one of four C_3 axes of **6**.

The exterior frame of **6** may be visualized as a twisted (to right or left) cuboctahedron **7**.^[7, 12] In Figure 1e, four tetrahedrally placed pink triangles represent **1** (pink balls at three triangle vertices are three Zn^{II} ions in **1**) and another tetrahedral set of four yellow triangles represent TCA^{3-} . In between, there are four rectangular planes. Cage **6** (or **7**)

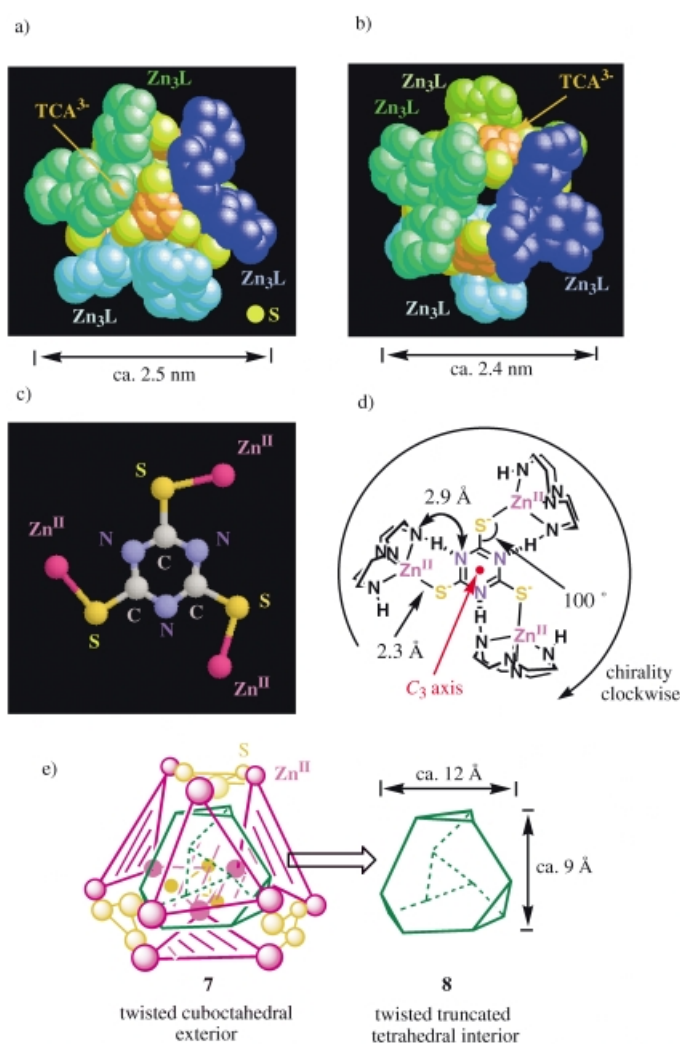


Figure 1. a, b) Space-filling drawings of the three-dimensional supramolecular complex **6** formed by 4:4 self-assembly of **1** and TCA and viewed a) along a C_3 -symmetry axis and b) along a C_2 -symmetry axis. The four molecules of **1** are light green, green, light blue, and blue; the 1,3,5-triazine rings of TCA^{3-} are orange, and the sulfur ions are yellow. All NO_3^- and H_2O are omitted; c, d) Ball and stick and graphical representation of bonding mode around TCA^{3-} in **6**; e) The exterior framework of **6** is represented as a twisted cuboctahedron **7** made of four triangular faces of **1** (purple triangles) and four triangular faces of TCA^{3-} units (yellow triangles). For clarity, cyclen rings are omitted. A green framework **8** is the inner cavity of **6**, as presented by a twisted truncated tetrahedron.

contains a distinct inner space, which is separated from the outer space by the four phenyl rings and four TCA^{3-} . The framework of the inner cavity is represented as a green polyhedron **8** (Figure 1e); this polyhedron is screwed clockwise at the four small triangles with respect to **5**. The interior space is about 12 Å wide and about 9 Å high.^[13] There are four rectangular pores (2×1 Å) at each edge of the tetrahedral framework.

Encapsulation of guests in the supramolecular cage 6: An interesting property of **6** is the encapsulation of organic guest compounds; we coincidentally discovered this property while measuring the 1H NMR spectrum of **6** in the presence of ($[D_4]$ -2,2,3,3)-3-(trimethylsilyl)propionic acid (TSP, for its structure, see Figure 3 later) as an internal standard reference

in D_2O (at $pD\ 7.0 \pm 0.2$ and $35^\circ C$). Figure 2a shows a very broad singlet for aromatic protons (all equivalent) of **1** (1.0 mM) at $\delta \sim 7.45$ with a TSP peak at $\delta = 0.00$ in solution at $pD\ 7.0$. A solution of crystalline **6** in D_2O (1.0 mM) in the absence of TSP gave a 1H NMR spectrum in which upfield

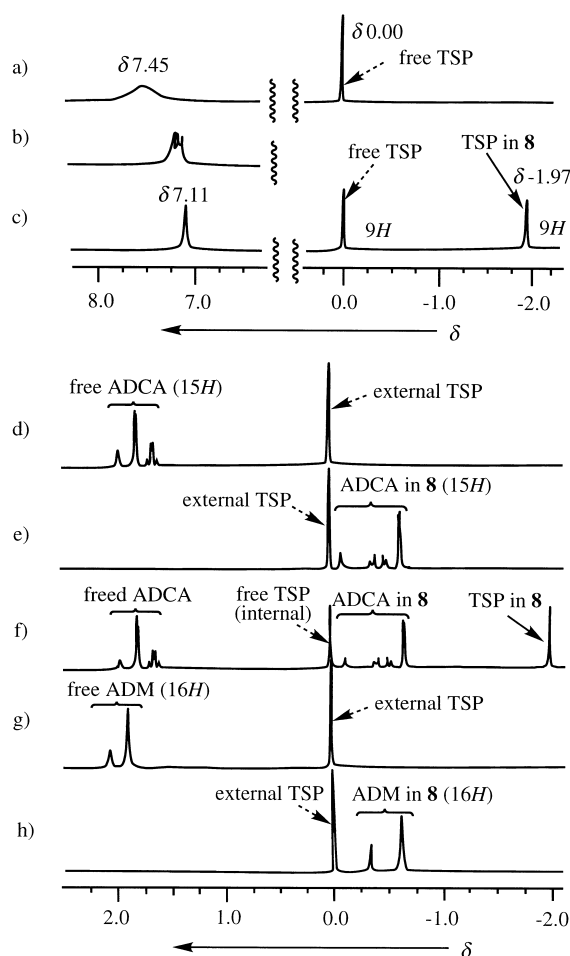


Figure 2. 1H NMR spectral changes in D_2O at $35^\circ C$; a) 1.0 mM **1** + 1.0 mM internal TSP at $pD\ 7.0$, b) 1.0 mM **6** at $pD\ 7.0$, c) 1.0 mM **6** + 2.0 mM internal TSP at $pD\ 7.0$, d) 0.5 mM ADCA at $pD\ 7.0$, e) 0.5 mM ADCA + 0.5 mM **6** at $pD\ 7.0$, f) spectrum obtained by addition of 0.5 mM TSP to the solution used to obtain the spectrum e, g) 1.0 mM ADM in $CDCl_3$, h) 1.0 mM **6** encapsulating equimolar ADM in D_2O at $pD\ 7.0$.

shifts for the aromatic protons to a multiplet at $\delta = 7.1 - 7.2$ were observed (Figure 2b); this might indicate several 1:1 (**1**:TCA) stoichiometric complex species equilibrating in aqueous solution. Addition of two equivalents of TSP (2.0 mM) rendered these multiplet aromatic protons to a sharp singlet at $\delta = 7.11$ (Figure 2c), indicating convergence to a sole 4:4 species **6**. In Figure 2c, half of the protons (9H) of TSP dramatically shift upfield to $\delta = -1.97$, a fact that suggests that one equimolar TSP was encapsulated in the inner cavity of **6** and is shielded from magnetic field by the surrounding aromatic rings. The remaining nine protons (as free TSP) stayed at the original $\delta = 0.0$. These facts together imply that the 4:4 assembly **6** becomes thermodynamically stable by inclusion of an equimolar amount of guest TSP.^[14] Moreover, the observation that the 1H singlet of the free TSP

and that of the encapsulated TSP appear as two distinct peaks indicates that the TSP-encapsulated complex is kinetically inert at least on the NMR timescale (400 or 500 MHz).^[7, 15–17]

The cavity **8** can also accommodate a molecule of 1-adamantanecarboxylic acid (ADCA) at pD 7.0; this was shown by an analogous upfield shift from $\delta = 1.7$ –2.1 for free ADCA (Figure 2d) to $\delta = -0.63$ –0.11 for the included species (Figure 2e). To see competition of ADCA and TSP for the cavity **8**, an equimolar amount of TSP was added to the solution that was used to obtain the spectrum shown in Figure 2e. The spectral change (Figure 2f) indicated that about half of the included ADCA was freed and that half of TSP went into **8**; this fact implies that the inclusion of ADCA and TSP is reversible, with both guests having similar inclusion affinities. We observed similar upfield shifts $\Delta\delta$ for adamantane (ADM) (see Figure 2g and h), 3-nitrophenol (3-NP), 4-nitrophenol (4-NP), 2,4-dinitrophenol (2,4-DNP), 2,4,6-collidine (2,4,6-CLD), 7-diethylaminocoumarin-3-carboxylic acid (DEACC), (*S*)-ibuprofen ((*S*)-IBP), [D]camphor ([D]CP), (1*S*,2*R*,4*R*)-2,10-camphorsultam ((1*S*,2*R*,4*R*)-CST),^[18] congressane (diadamantane, CGS),^[19] (1*R*,2*S*,5*S*)-(-)-menthoxyacetic acid ((1*R*,2*S*,5*S*)-MAA), the tetraethylammonium (TEA) cation, and the tetra-*n*-propylammonium (TPA) cation in D₂O at pD 7.0 ± 0.2 and 35 °C (for structures and $\Delta\delta$ values, see Figure 3).^[20, 21] On the other hand, amantadine (AMT, 1-aminoadamantane), (1*S*)-camphorsulfonic acid ((1*S*)-CSA), the tetramethylammonium (TMA) cation, and the tetra-*n*-butylammonium (TBA) cation did not show such ¹H upfield shifts, indicating that these were not included.

To account for the requirements for these guests in **8**, we tested partition of the potential guest molecules (2.0 mM) from a D₂O solution (pD 7.0 ± 0.2) into 1-octanol (D₂O:1-octanol = 1:1 (v/v)). As summarized in Table 1, the non-guests AMT,^[22] (1*S*)-CSA, and TMA remained more in aqueous phase, while the guest molecules were better partitioned into the organic phase. Judging from the p*K*_a values for the acid–base functions of the organic molecules tested (Figure 3), the guests are either anionic (–CO₂[–]) or neutral, while the non-guests are cationic (–NH₃⁺). The lipophilic tetra-*n*-butylammonium (TBA) cation and tetraphenylborate (TPB) anion were not encapsulated, possibly because of their steric bulkiness. Therefore, it was concluded that the supramolecular capsule **6** with cationic exterior accommodates neutral or anionic hydrophobic molecules or size-matched quaternary ammonium molecules.^[23]

Crystal structure of the 6–adamantane (6-ADM) inclusion complex:

The 1:1 6-ADM complex was crystallized out from the mixed solution at pH 8.0. The single-crystal X-ray structure has proven the encapsulation of ADM in the matching size of the inner cavity **8**. The crystal data are summarized in the Experimental Section.^[24] Figure 4a is a space-filling drawing of the central core of the 6-ADM complex. The guest ADM (red) is surrounded by the four phenyl rings of **1** (light green, green, light blue, and blue) from one set of triangular tetrahedral faces and by the four TCA^{3–} aromatic rings (orange) from the other set of tetrahedral faces. As shown in Figure 4b (a blue phenyl ring from the front is omitted for clarity), the four cyclohexane rings framing

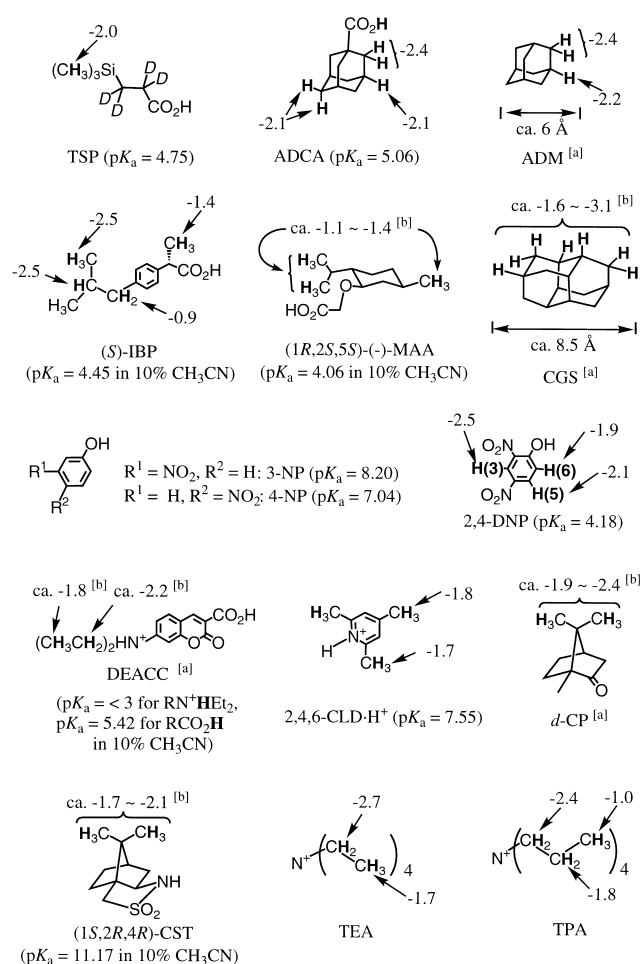


Figure 3. Organic guest molecules with the $\Delta\delta$ values (ppm) upon encapsulation in D₂O at pD 7.0 ± 0.2 and 35 °C. [a] The δ values are compared with those of free guests in CDCl₃. [b] Approximate $\Delta\delta$ values are listed due to difficult assignment of peaks or broadening peaks of the included guests).

Table 1. The encapsulation of organic molecules in **6** (=inner cavity **8**).

| organic molecule | encapsulation in 6 ^[a,d] | log <i>K</i> _{enc} ^[b,d] | partition to 1-octanol (%) ^[c,d] |
|---|--|--|---|
| TSP | yes | 5.7 ^[e] | 34 |
| ADCA | yes | 5.5 ^[e] | 35 |
| AMT | no | – | negligible |
| ADM | yes | n.d. ^[f] | n.d. |
| 4-NP | yes | 5.2 ^[g] | n.d. |
| 2,4-DNP | yes | 6.0 ^[g] | 21 |
| DEACC | yes | 6.1 ^[g] | n.d. |
| 2,4,6-CLD | yes | n.d. | 17 |
| TMA | no | – | negligible |
| TEA | yes | n.d. | 15 (13) ^[h] |
| TPA | yes | 5.4 ^[e] | 11 (12) ^[h] |
| TBA | no | – | 12 |
| (1 <i>S</i> ,2 <i>R</i> ,4 <i>R</i>)-CST | yes | n.d. | > 97 |
| (1 <i>S</i>)-CSA | no | – | negligible |

[a] Determined by ¹H NMR experiments in D₂O at pD 7.0 ± 0.2. [b] Determined by UV titrations in D₂O at pD 7.0 (50 mM HEPES with *I* = 0.1 (NaNO₃)) and 25 °C. For definition, see the text and ref. [30]. [c] Partition yields from D₂O solution (initial concentration of compounds were 2 mM and initial pD's were 7.0 ± 0.2) into 1-octanol (D₂O:1-octanol = 1:1 (v/v)). Experimental errors are ± 3%. [d] The experiments were repeated twice or three times. [e] Experimental errors are ± 0.3. [f] n.d. = not determined. [g] Experimental errors are ± 0.1. [h] Values in parentheses are partition yields in the presence of 200 mM NaCl.

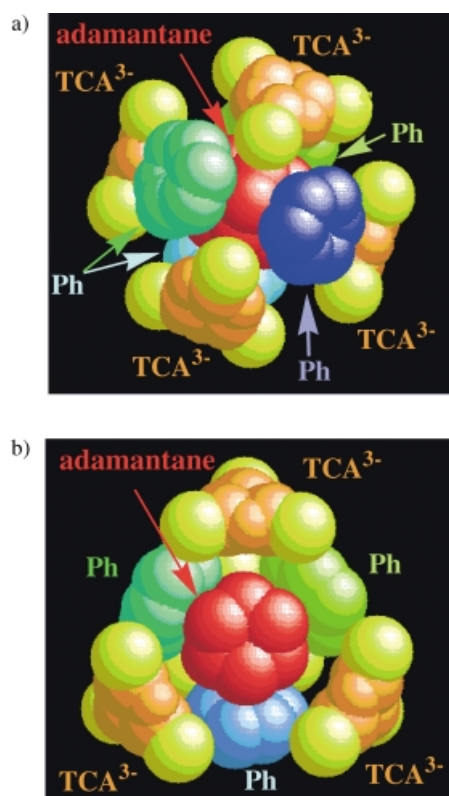


Figure 4. a) Space-filling drawing of central core of the **6**-ADM complex, showing ADM in red surrounded by four (light blue, blue, light green, and green) phenyl rings from the cyclen ligand “tetrahedron” and more remotely by the four TCA^{3-} rings; b) Each of four cyclohexane rings that constitute the ADM molecule face a phenyl ring (the forefront phenyl ring is omitted for clarity).

ADM squarely face the tetrahedrally surrounding phenyl rings.

An interesting finding of the **6**-ADM complex was that ADM, unlike ADCA, was not liberated from the cavity upon addition of two equivalents TSP in D_2O at pD 7.0 and 35°C .^[25] Alternatively, when the **6**-TSP complex was stirred with excess ADM (added as insoluble solids) at pD 7.0 and 35°C , the encapsulated TSP was completely displaced by ADM. It was concluded that the **6**-ADM complex is kinetically and/or thermodynamically more stable than the **6**-TSP complex.^[26]

Determination of the 4:4 self-assembly constants by potentiometric pH and UV spectrophotometric titrations: We examined the pH-dependent self-assembly of **1** (1.0 mM) with TCA (1.0 mM) by potentiometric pH titrations in the presence of excess tetra-*n*-propylammonium (TPA) bromide^[27] at 25°C with $I = 0.1$ (NaNO_3). Figure 5a shows the titration curves for **1**, TCA, and **1** + TCA in the absence and presence of TPA. The last titration curve (curve d) indicates that all the three protons of TCA were deprotonated by pH 6. Note that the complete deprotonation of TCA alone required $\text{pH} > 12$ (see Scheme 2). Analysis of the last pH titration curve with the program BEST^[28] gave a fit to the 4:4 complexation scheme with a $\log K_{\text{app}}$ value [defined by Eqs. (4)–(6)] of 34.0 ± 2.0 at pH 7.0. In the absence of TPA, the third deprotonation of TCA occurred as well, but analysis for the 4:4 complex

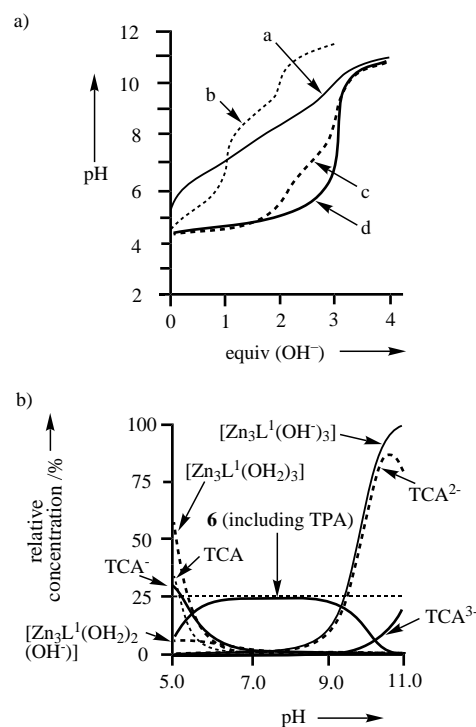


Figure 5. a) The pH titration curves for a) 1.0 mM **1**, b) 1.0 mM TCA, c) 1.0 mM **1** + 1.0 mM TCA, and d) 1.0 mM **1** + 1.0 mM TCA + 1.0 mM TPA at 25°C with $I = 0.10$ (NaNO_3); b) Speciation diagram calculated for 1.0 mM **1**/1.0 mM TCA/1.0 mM TPA mixture as a function of pH at 25°C with $I = 0.10$ (NaNO_3). For clarity, the species less than 5% were omitted.

scenario was not successful. Figure 5b is a pH-dependent speciation diagram for a mixture of **1** (1.0 mM) and TCA (1.0 mM) in the presence of TPA (1.0 mM) and demonstrates that the 4:4 supramolecular capsule **6** (including a TPA guest) is formed in over 95% yield at $6.3 < \text{pH} < 8.7$.

$$K_{\text{app}} = [\mathbf{6}\text{-TPA}]/[\mathbf{1}]^4[\text{TCA}]^4 \text{ (M}^{-7}\text{)} \quad (4)$$

$$[\mathbf{1}] = [\mathbf{1} \cdot (\text{H}_2\text{O})_3]_{\text{free}} + [\mathbf{1} \cdot (\text{H}_2\text{O})_2(\text{HO}^-)]_{\text{free}} + [\mathbf{1} \cdot (\text{H}_2\text{O})(\text{HO}^-)_2]_{\text{free}} + [\mathbf{1} \cdot (\text{HO}^-)_3]_{\text{free}} \quad (5)$$

$$[\text{TCA}] = [\text{TCA}]_{\text{free}} + [\text{TCA}^-]_{\text{free}} + [\text{TCA}^{2-}]_{\text{free}} + [\text{TCA}^{3-}]_{\text{free}} \quad (6)$$

The UV spectrophotometric titration of TCA ($30 \mu\text{M}$; $\lambda_{\text{max}} = 283 \text{ nm}$, $\epsilon = 4.1 \times 10^4 \text{ M}^{-1} \text{ cm}^{-1}$ and $\lambda_{\text{max}} = 323 \text{ nm}$, $\epsilon = 2.8 \times 10^4 \text{ M}^{-1} \text{ cm}^{-1}$ at pH 7.0) with **1** was conducted in the presence of TPA (0.1 mM) in HEPES^[29] (50 mM, pH 7.0 with $I = 0.1$ (NaNO_3)) at 25°C , as shown in Figure 6. The inset is the decreasing ϵ_{323} with increasing **1** (where equiv(**1**) is the number of equivalents of **1** against TCA) from which $\log K_{\text{app}}$ was calculated to be 35.5 ± 3.0 , which is close to the value determined by the above potentiometric pH titration.

Determination of the encapsulation constants of guest molecules: The UV spectrophotometric titrations of 4-NP, 2,4-DNP, 2,4,6-TNP, and DEACC (all $50 \mu\text{M}$) with **6** at pH 7.0 (50 mM HEPES with $I = 0.1$ (NaNO_3)) and 25°C were carried out to determine the 1:1 host–guest complexation constants. Figure 7 represents the titration of 2,4-DNP ($50 \mu\text{M}$) with **6**, which was prepared in situ by adding TCA (0–0.1 mM) to a

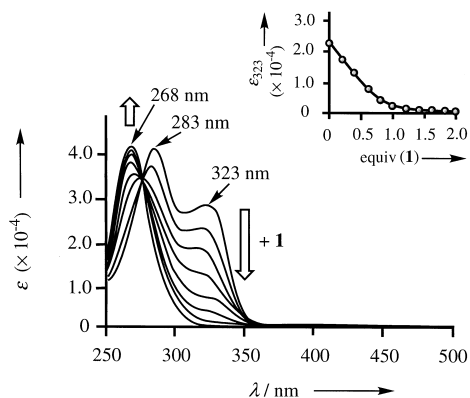


Figure 6. UV absorption spectral change of TCA (30 μM) upon addition of **1** in the presence of TPA (0.1 mM) in HEPES (50 mM, pH 7.0 with $I=0.1$ (NaNO_3)) at 25 $^\circ\text{C}$. The inset shows decreasing absorbances at 323 nm (ϵ_{323}) upon addition of **1**.

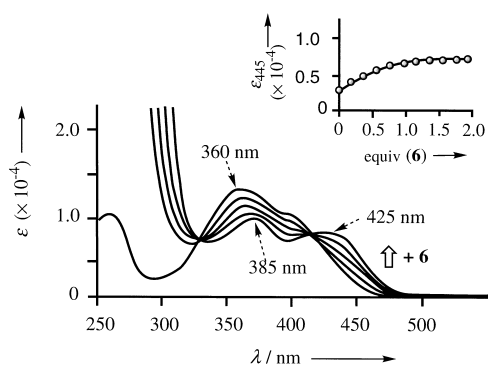


Figure 7. The UV titration of 2,4-DNP (50 μM) with **6** in aqueous solution at pH 7.0 (50 mM HEPES with $I=0.1$ (NaNO_3)) and 25 $^\circ\text{C}$. The inset is increasing absorbance at 445 nm (ϵ_{445}) by addition of **6**, from which the encapsulation constant, K_{enc} , of 2,4-DNP with **6** was calculated.

large excess of **1** (1.0 mM) (so that **6** is formed almost quantitatively). From the increasing curve of ϵ_{445} as shown in the inset, the apparent encapsulation constant, $\log K_{\text{enc}}$ [defined by Eq. (7)]^[30] of 2,4-DNP in **6** was calculated to be 6.0 ± 0.1 . The host **6** had negligible UV absorption above 400 nm. Similarly, the $\log K_{\text{enc}}$ values of 4-NP, 2,4,6-TNP, and DEACC were determined and are summarized in Table 1.

$$K_{\text{enc}} = [\mathbf{6}\text{-guest}]/[\mathbf{6}][\text{guest}] \quad (\text{M}^{-1}) \quad (7)$$

An unexpected finding was that the UV absorption spectrum of the encapsulated 2,4-DNP showed a 22–27 nm bathochromic (red) shift with respect to that of the free 2,4-DNP. It is suspected that 2,4-DNP, which has highly electron-deficient moieties, may form π – π stacks with the aromatic groups of **6** or may be somehow in a more conjugated form. The encapsulation constants of TSP, ADCA, and TPA in **6** were estimated by the competitive displacement of 2,4-DNP by these guests at pH 7.0 (50 mM HEPES with $I=0.1$ (NaNO_3)) and 25 $^\circ\text{C}$. The results are listed in Table 1.^[31]

Measurement of hydrophobicity of the inner cavity 8: On the basis of the guest molecular recognition properties of **6**, we concluded that the inner cavity **8** should be hydrophobic. Its hydrophobicity was qualitatively measured by the fluores-

cence intensity of the encapsulated fluorophore 7-diethylaminocoumarin-1-carboxylic (DEACC, 20 μM) at pH 7.0 (10 mM HEPES with $I=0.1$ (NaNO_3)) and 25 $^\circ\text{C}$. Empirically, the emission intensity of DEACC increases in more hydrophobic environment.^[32] The excitation of free DEACC (see Figure 3 for structure) at 374 nm (the isosbestic absorption point determined by UV titration) gave the quantum yields (Φ) of 0.04 ± 0.01 in H_2O (emission maxima at 472 nm), 0.17 ± 0.01 in methanol, 0.22 ± 0.01 in 2-propanol, 0.23 ± 0.01 in 85:15 (v/v) 1,4-dioxane/ H_2O , 0.60 ± 0.01 in 1-octanol, and 0.69 ± 0.01 in 1,4-dioxane (emission maxima at 456 nm) (Figure 8). Since DEACC in the cage cavity **8** gave $\Phi = 0.24 \pm 0.01$, we estimate the hydrophobicity of the inner cavity **8** to be close to that of 2-propanol or 85:15 (v/v) 1,4-dioxane/ H_2O .^[33]

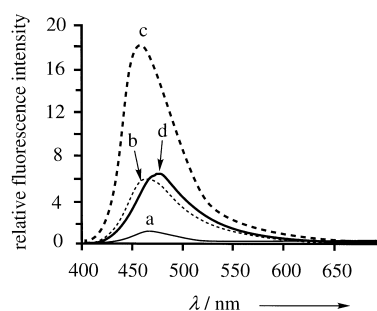
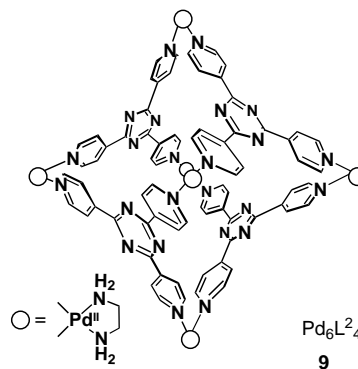


Figure 8. Fluorescence emission spectra of 20 μM DEACC a) in HEPES (10 mM, pH 7.0 with $I=0.1$ (NaNO_3)), b) in 2-propanol, and c) in 1,4-dioxane. The emission of DEACC (20 μM) encapsulated in **6** gave a curve d, whose quantum yield (Φ) is 0.24.

Comparison of encapsulation properties of 6 with other host molecules: Encapsulation of hydrophobic guests by **6** were compared with those of cyclodextrins (CDs)^[34] and Fujita's supramolecular cage **9** ($[\text{Pd}_6\text{L}_2^4]$), which is composed of four 2,4,6-tri(4-pyridyl)-1,3,5-triazine (L^2) units and six palladium(II) ions.^[35] Both CDs and **9** can include common guests such as ADCA.



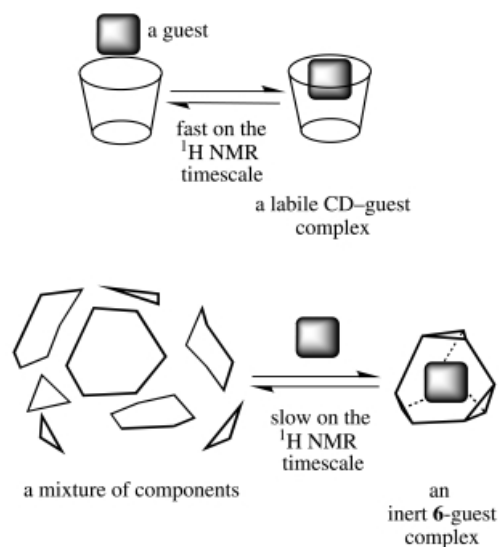
The calculated apparent encapsulation constant, $\log K_{\text{enc}}$, of 5.2 ± 0.1 for **6**-4-NP is greater than the reported $\log K_{\text{enc}}$ values for α -CD-4-NP complex (2.6 at pH 3.5 and 3.6 at pH 11).^[36] The aromatic proton signals of 4-NP in the **6**-4-NP complex (1 mM) did not change upon addition of α -CD (1 mM) at pH 7.0 in D_2O . On the other hand, upon addition of equivalent amount of **6** to the α -CD-4-NP complex, most of

4-NP went into **6**, a fact supporting the much higher thermodynamic stability of **6**-4-NP. When α -CD (100 mM) was added to the **6**-4-NP complex (1 mM), about a half of 4-NP moved into the inner cavity of α -CD, as suggested from the $\log K_{\text{enc}}$ constants.

The complexation constant ($\log K_{\text{enc}}$) of 4.8 was reported for β -CD-ADCA in aqueous solution at pH 7.2.^[37] The ^1H NMR spectrum of ADCA (1.0 mM) in D_2O at pD 7.0 \pm 0.1 and 35 °C in the presence of β -CD (1.0 mM) showed the averaged ^1H signals of free ADCA and encapsulated ADCA in β -CD with downfield shifts of $\delta = 0.11$ –0.14; this indicates that the β -CD-ADCA complex is kinetically labile on the ^1H NMR timescale. This was in sharp contrast to the inert complex between **6** and ADCA.

Fujita's supramolecular cage **9** was reported to encapsulate four molecules of ADCA in aqueous solution,^[35] but the encapsulation constants of **9** were not reported. Direct comparison of the ADCA affinities of **9** with those of **6** was not possible, due to the formation of yellow precipitates when the **9**-(ADCA)₄ was mixed with four equivalents **6** in D_2O at pD 7.0. Instead, four equivalents of β -CD were added to the **9**-(ADCA)₄ complex (1 mM) in D_2O at pD 7.0, and we found that only about 15% of the ADCA was removed to the inner cavity of β -CD. On the other hand, upon addition of β -CD (1 mM) to the **6**-ADCA complex (1 mM) in D_2O at pD 7.0, approximately 33% of ADCA moved into the β -CD.^[38, 39] Therefore, we assume that the ADCA inclusion affinity order is **9**-(ADCA)₄ > **6**-ADCA > β -CD-ADCA.

Our assumption of the encapsulation mode of CDs and the supramolecular cage **6** is illustrated in Scheme 3. Equilibria of the CD–guest complexes are fast on the ^1H NMR timescale,



Scheme 3.

because of the wide “entrance” of CD. On the other hand, the entrance of **6** is too narrow (see the X-ray crystal structure results) to let a guest molecule out. However, during slow (on the ^1H NMR timescale) equilibration of **6** between a mixture of components and 4:4 self assembly, a hydrophobic and size-matched guest is encapsulated and released.

The deprotonation constants of encapsulated acids in the inner cavity 8: We measured the $\text{p}K_{\text{a}}$ values of 4-NP in the relatively hydrophobic cavity **8** under the conditions for which 4-NP is almost completely encapsulated in **6**, as known from the previous K_{enc} values. The typical titration curve of 4-NP (0.5 mM, $\text{p}K_{\text{a}} = 7.04 \pm 0.05$ in unencapsulated state) in the presence of **6** (0.25 mM) at 25 °C with $I = 0.1$ (NaNO_3) revealed two $\text{p}K_{\text{a}}$ values; the lower value of 7.0 ± 0.1 for the free unencapsulated 4-NP and the higher value of 8.2 ± 0.1 for the encapsulated 4-NP. The result led us to conclude that 4-NP prefers to remain neutral by raising the $\text{p}K_{\text{a}}$ value in the aprotic environment in **8**. The weak base 2,4,6-CLD ($\text{p}K_{\text{a}} = 7.55 \pm 0.05$) became weaker in **8** with the $\text{p}K_{\text{a}}$ value of 6.6 ± 0.1 , because it also prefers to stay neutral in aprotic **8**. These results support that the nonionic, neutral forms of guest molecules are more stabilized in the hydrophobic **8**.^[40, 41] Encapsulated complexes of neutral 3-NP, anionic 4-NP⁻, and 2,4-DNP⁻ were isolated as crystals from an aqueous solutions at pH 7–8 (see the Supporting Information).

Circular dichroism spectra of the supermolecule **6** with encapsulated chiral guests:

As described above, **6** is a chiral supermolecule due to the asymmetric arrangement of Zn^{II} -cyclen units around TCA^{3-} (Figure 1c and d). The X-ray analysis showed that each crystal of **6** and **6**-ADM contained either of two enantiomers, indicating that crystals as a whole are *racemic mixture (conglomerate)*.^[42] It was interesting to see if the supramolecular chirality is influenced by a chiral guest molecule. From the ^1H NMR study, we found (1*S*,2*R*,4*R*)-(-)-camphorsultam ((1*S*,2*R*,4*R*)-(-)-CST) to be an appropriate guest molecule. The circular dichroism spectrum of **6** (0.2 mM) in aqueous solution at pH 7.0 \pm 0.1 and 25 °C gave a negative Cotton effect at 262 nm ($\Delta\epsilon = -24 \text{ M}^{-1} \text{ cm}^{-1}$) and a positive Cotton effect at 224 nm ($\Delta\epsilon = +24$) upon addition of (1*S*,2*R*,4*R*)-(-)-CST (0.2 mM; curve a in Figure 9, amplitude = -48). An exact mirror image was obtained by addition of the (1*R*,2*S*,4*S*)-(+)-CST enantiomer (0.2 mM, curve b). Addition of racemic CST yielded negligible Cotton effects (curve c). The Cotton effects disappeared upon decomposition of **6** by addition of OH^- . These facts together indicate that an inner chiral guest can control the exterior chirality of **6**.^[43] Curves d and e are circular dichroism spectra

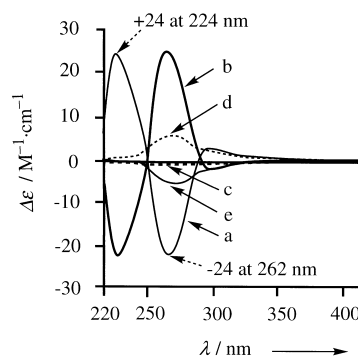


Figure 9. Circular dichroism spectra of **6** (0.2 mM) in the presence of an equimolar amount of a) (1*S*,2*R*,4*R*)-(-)-CST, b) (1*R*,2*S*,4*S*)-(+)-CST, c) racemic CST, d) (-)-MAA, and e) (+)-MAA in H_2O (pH 7.0 \pm 0.1) at 25 °C.

of **6** (0.2 mM) in the presence of (1*R*,2*S*,5*S*)-(–)-menthoxyacetic acid ((1*R*,2*S*,5*S*)-(–)-MAA) and its enantiomer (1*S*,2*R*,5*R*)-(+)MAA (0.2 mM). The Cotton effects at 262 nm are less significant with respect to those of curves a and b, probably because of less rigid host–guest interaction. The extent of an enantiomeric excess and absolute configuration of **6** induced by the chiral guests remains to be studied.^[44, 45]

Conclusion

We have discovered a novel 4:4 self-assembly of tris(Zn^{II}-cyclen) complex **1** and tri-deprotonated trithiocyanuric acid (TCA³⁻) in neutral aqueous solution. The resulting supermolecule **6** was isolated and characterized by X-ray crystal structure analysis, pH-metric and UV spectrophotometric titrations, and ¹H NMR spectroscopy. The new cage complex **6** has unique properties:

- 1) It is thermodynamically stable and forms quantitatively through the formation Zn²⁺–S⁻(exocyclic) bonds at [1] = [TCA] = 1.0 mM in the presence of a guest molecule in aqueous solution at neutral pH.
- 2) The three-dimensional exterior may be viewed as a cuboctahedral architecture **7**.
- 3) It has a discrete nanoscale inner hollow (truncated tetrahedral cage) **8** separated from exterior by four phenyl rings of **1** and four 1,3,5-triazine rings of TCA³⁻. The inner cavity **8** encapsulates hydrophobic and size-matching organic guests such as TSP, ADCA, 3-NP, 4-NP, 2,4-DNP, ADM, TEA, or TPA [with K_d (= $1/K_{enc}$) values of μM order].
- 4) The self-assembled **6** and its guest-including complexes are kinetically stable (on the NMR timescale); however, the guest molecules in **8** can be exchanged (except for ADM).
- 5) The polarity of the inner space **8** is estimated to be near to that of 2-propanol by means of fluorescence measurements of the encapsulated DEACC.
- 6) The ADCA inclusion affinity of **6**-ADCA is between those of **9**-(ADCA)₄ and β -CD-ADCA in aqueous solution.
- 7) In the hydrophobic cavity **8**, 4-NP and 2,4,6-CLD prefer to take neutral forms, resulting in higher pK_a values for 4-NP and a lower pK_a value for 2,4,6-CLD · H⁺.
- 8) The exterior superstructure is chiral. Cage **6** is optically inactive when it encapsulates achiral guests; however, enantiomeric **6** was attained from within by encapsulation of enantiomeric guests.

The present new construction method of a supramolecular capsule with a unique inner cavity should be versatile and useful for molecular recognition or reaction phases in aqueous solution.

Experimental Section

General information: TSP sodium salt, ADCA, AMT, CGS, DEACC, [D]CP, (*S*)-IBP, (1*S*)-CSA, (1*S*,2*R*,4*R*)-(–)-CST, (1*R*,2*S*,4*S*)-(+)CST, (1*R*,2*S*,5*S*)-(–)-MAA, (1*S*,2*R*,5*R*)-(+)MAA, TMA chloride, TEA chloride, TPA bromide, TBA bromide, and sodium TPB were of the highest commercial quality and used without further purification. TCA, ADM,

3-NP, 4-NP, 2,4-DNP, and 2,4,6-CLD · HCl (prepared from 2,4,6-CLD and aq. HCl) were recrystallized and their purity was determined by potentiometric pH titration. The supramolecular cage **9** ([Pd₆L₂]₄) was kindly provided by Professor Makoto Fujita, Nagoya University. All aqueous solutions were prepared with using deionized and redistilled water. The HEPES (2-[4-(2-hydroxyethyl)-1-piperazinyl]ethanesulfonic acid, pK_a = 7.6 at 25 °C) buffer was purchased from Dojindo Laboratories and used without further purification. Melting points were measured on Yanaco melting-point apparatus and listed without correlation. IR spectra were recorded on a Horiba Fourier transform infrared spectrometer FT-710. ¹H and ¹³C NMR spectra were recorded on a JEOL Alpha (400 MHz) or Lambda (500 MHz) spectrometer. TSP in D₂O and 1,4-dioxane were used as external references of ¹H NMR and ¹³C NMR experiments, respectively, except when TSP was added as a guest molecule. The pD values in D₂O were corrected for a deuterium isotope effect using pD = pH + 0.40. Elemental analysis was performed on a Perkin–Elmer CHN Analyzer 2400. UV spectra and fluorescence emission spectra were recorded on a Hitachi U-3500 spectrophotometer and a Hitachi F-4500 fluorescence spectrophotometer, respectively, at 25.0 ± 0.1 °C. The obtained data from UV titrations were analyzed for apparent complexation constants (K_{app}) and encapsulation constants (K_{enc}) by using the program Bind Works (Calorimetry Sciences). Quantum yields of fluorescence emission were determined by comparison of the integrated corrected emission spectrum of a standard quinine (excitation at 335 nm was used for quinine in 0.10 M H₂SO₄, whose quantum yield was 0.54). Circular dichroism spectra were recorded on a JASCO J-720 spectropolarimeter.

Isolation of 6[NO₃]₁₂ · 22H₂O: Complex 1[NO₃]₆ · 3H₂O · 0.5EtOH^[8] (385 mg, 0.30 mmol), trithiocyanuric acid (53 mg, 0.30 mmol), and NaNO₃ (0.25 g, 30 mm) were dissolved in H₂O (30 mL), and the pH was adjusted to pH 8.0 by addition of aqueous NaOH. The whole mixture was filtered and concentrated slowly in vacuo for a week, and colorless prisms of 6[NO₃]₁₂ · 22H₂O (270 mg, 70% yield) were obtained. M.p. > 250 °C; ¹H NMR (400 MHz, CD₃CN/D₂O (10/90), 35 °C, external TSP): δ = 2.63–3.20 (m, 168 H, CH₂ of cyclen rings), 3.33–3.45 (m, 24 H, CH₂ of cyclen rings), 4.06 (brs, 24 H, ArCH₂), 4.20 (br, NH), 7.19 (brs, 12 H, ArH); ¹³C NMR (125 MHz, CD₃CN/D₂O (10/90), 35 °C, external 1,4-dioxane): δ = 43.42, 45.08, 45.52, 50.09, 56.28, 133.42, 134.27, 184.64; IR (KBr): $\tilde{\nu}$ = 3788, 3460, 3223, 2924, 2875, 1630, 1430, 1384, 1229 cm⁻¹; elemental analysis calcd (%) for C₁₄₄H₃₀₈N₇₂O₅₈S₁₂Zn₁₂: C 33.61, H 6.03, N 19.60; found: C 33.64, H 6.31, N 19.33.

Isolation of 6-ADM[NO₃]₁₂ · 27H₂O: Complex 6[NO₃]₁₂ · 22H₂O (129 mg, 0.025 mmol) and NaNO₃ (0.34 g, 4.0 mm) were dissolved in H₂O (30 mL), to which adamantane (32 mg, 0.23 mmol) was added, and the resulting mixture was vigorously stirred at 40 °C overnight. The whole mixture was filtered and concentrated slowly in vacuo. The resulting colorless powders were recrystallized from H₂O and dried in vacuo at room temperature to give colorless prisms of 6-ADM[NO₃]₁₂ · 27H₂O (110 mg, 82% yield). M.p. > 250 °C; ¹H NMR (400 MHz, D₂O, 35 °C, external TSP): δ = –0.60 (m, 12 H, CH₂ of ADM), –0.33 (m, 4 H, CH of ADM), 2.65–3.62 (m, 192 H, CH₂ of cyclen rings), 3.97 (brs, 24 H, ArCH₂), 4.15 (brs, 12 H, NH), 7.13 (brs, 12 H, ArH); ¹³C NMR (125 MHz, D₂O, 35 °C, external 1,4-dioxane): δ = 26.06, 33.67, 41.87, 42.24, 43.46, 43.75, 44.17, 48.86, 132.11, 133.16, 182.75; IR (KBr): $\tilde{\nu}$ = 3433, 3261, 2927, 2879, 2424, 2360, 1635, 1437, 1383, 1232, 1090, 970, 845 cm⁻¹; elemental analysis calcd (%) for C₁₅₄H₃₃₀N₇₂O₆₃S₁₂Zn₁₂: C 34.46, H 6.20, N 18.79; found: C 34.16, H 6.15, N 19.11.

Crystallographic study of 6[NO₃]₁₂ · 22H₂O: A colorless prismatic crystal of 6[NO₃]₁₂ · 22H₂O (C₁₄₄H₃₀₈N₇₂O₅₆S₁₂Zn₁₂, M_r = 5145.75) with approximate dimensions of 0.35 × 0.20 × 0.10 mm was mounted in a loop. Intensity data were collected on a Rigaku RAXIS-RAPID imaging-plate diffractometer with MoK α radiation at a temperature of –160 ± 1 °C. Cell constants and an orientation matrix for data collection corresponded to F-centered cubic cell (Laue class : m3m) with dimensions: a = 39.182(1) Å, V = 60153(3) Å³. For Z = 8 and M_r = 5107.71, the calculated density (ρ_{calcd}) is 1.14 g cm⁻³. Based on the systematic absence of: hkl : $h + k$, $k + lm$, $h + l \neq 2n$, packing considerations, a statistical analysis of intensity distribution, and the successful solution and refinement of the structure, the space group was determined to be $F432$ (No. 209). A total of 108 images, corresponding to 220.0° oscillation angles, were collected with two different goniometer settings. Data were processed by the PROCESS-AUTO program package. Of the 93056 reflections which were collected, 1883 were unique (R_{int} =

0.018); equivalent reflections were merged. The linear absorption coefficient, μ , for $\text{MoK}\alpha$ radiation was 10.9 cm^{-1} . A symmetry-related absorption correction using the program ABCOR was applied; this resulted in transmission factors ranging from 0.59 to 0.90. The structure was solved by direct methods (SHELXS-86) and expanded by means of Fourier techniques (DIRDIF-94). The reflections in the range of 2θ between 15.0° and 45.0° were used for the structure refinement: the spots recorded at the lower angles were overlapped by those diffracted from adhered crystalline particles. The atoms of the cation were located and refined as usual, but the O atoms of NO_3 anions, apart from those of three of a total twelve anions, were not located. The final cycle of full-matrix least-squares refinement (SHELXL-97) was based on 1121 observed reflections [$I > 2\sigma(I)$] and 154 variable parameters and converged (largest parameter shift was -0.01 times its esd) with unweighted and weighted agreement factors of: $R = \Sigma(F_o^2 - F_c^2)/\Sigma F_o^2 = 0.100$. $R_w = [\Sigma w(F_o^2 - F_c^2)^2/\Sigma w(F_o^2)^2]^{0.5} = 0.259$. The standard deviation of an observation of unit weight was 1.20. The maximum and minimum peaks on the final difference Fourier map corresponded to 0.55 and $-0.53 \text{ e}\text{\AA}^{-3}$, respectively. All calculations were performed with the teXsan crystallographic software package of the Molecular Structure Corporation (1985, 1999).

Crystallographic study of 6-ADM[NO₃]₁₂·27H₂O: A colorless prismatic crystal of 6-ADM[NO₃]₁₂·27H₂O ($\text{C}_{154}\text{H}_{334}\text{N}_{72}\text{O}_{63}\text{S}_{12}\text{Zn}_{12}$, $M_r = 5372.06$) with approximate dimensions of $0.50 \times 0.50 \times 0.25 \text{ mm}$ was mounted in a loop. Intensity data were collected on a Rigaku RAXIS-RAPID imaging plate diffractometer with $\text{MoK}\alpha$ radiation at a temperature of $-150 \pm 1^\circ\text{C}$. Indexing was performed from two oscillations which were exposed for 8.0 minutes. Cell constants and an orientation matrix for data collection corresponded to an F-centered cubic cell (Laue class: m3m) with dimensions: $a = 39.061(1) \text{ \AA}$, $V = 59599(3) \text{ \AA}^3$. For $Z = 8$ and $M_r = 5372.06$, the calculated density (ρ_{calcd}) was 1.20 g cm^{-3} . Based on the systematic absence of: $hkl: h + k, k + l, h + l \neq 2n$, packing considerations, a statistical analysis of intensity distribution, and the successful solution and refinement of the structure, the space group was determined to be: F432 (No. 209). A total of 110 images, corresponding to 220.0 K oscillations angles, were collected with two different goniometer settings. Data were processed by the PROCESS-AUTO program package. Of the 96683 reflections which were collected, 1331 were unique ($R_{\text{int}} = 0.077$); equivalent reflections were merged. The linear absorption coefficient, μ for $\text{MoK}\alpha$ radiation was 11.0 cm^{-1} . A symmetry-related absorption correction using the program ABCOR was applied which resulted in transmission factors ranging from 0.62 to 0.76. The data were corrected for Lorentz and polarization effects. The structure was solved by direct methods (SHELXS86) and expanded by means of Fourier techniques (DIRDIF 94). The reflections in the range of 2θ between 15.0° and 40.0° were used for the structure refinement: the spots recorded at the lower angles were overlapped by those diffracted from adhered crystalline particles. The atoms of the cation were located and refined as usual, but the O atoms of NO_3 ions, apart from those of three of a total twelve anions, were not located. This is probably due to disordered structures exhibited by the anions in which the N atoms lie on symmetry elements in the crystal. The final cycle of full-matrix least-squares refinement (SHELXL-97) was based on 752 observed reflections [$I > 2\sigma(I)$] and 156 variable parameters and converged (largest parameter shift was -0.01 times its esd) with unweighted and weighted agreement factors of: $R = \Sigma(F_o^2 - F_c^2)/\Sigma F_o^2 = 0.103$. $R_w = [\Sigma w(F_o^2 - F_c^2)^2/\Sigma w(F_o^2)^2]^{0.5} = 0.263$. The standard deviation of an observation of unit weight was 1.30. The maximum and minimum peaks on the final difference Fourier map corresponded to 0.33 and $-0.26 \text{ e}\text{\AA}^{-3}$, respectively.

Crystallographic data (excluding structure factors) for the structures reported in this paper have been deposited with the Cambridge Crystallographic Data Centre as supplementary publication nos. CCDC-170091 (6) and CCDC-170092 (6-ADM). Copies of the data can be obtained free of charge on application to CCDC, 12 Union Road, Cambridge CB2 1EZ, UK (fax: (+44) 1223-336-033; e-mail: deposit@ccdc.cam.ac.uk).

Potentiometric pH titrations: The preparation of the test solutions and the calibration method of the electrode system [Potentiometric Automatic Titrator AT-400 and Auto Piston Buret APB-410 (Kyoto Electronics Manufacturing.) with Orion Research Ross Combination pH Electrode 8102BN] were described earlier.^[6–8, 15] All the test solutions (50 mL) were kept under an argon (>99.999% purity) atmosphere. The potentiometric pH titrations were carried out with $I = 0.10$ (NaNO_3) at $25.0 \pm 0.1^\circ\text{C}$ (0.1 N

NaOH was used as a base), and at least two independent titrations were performed. Deprotonation constants of Zn^{2+} -bound water $K'_2 = [\text{HO}^- \text{-bound species}][\text{H}^+]/[\text{H}_2\text{O-bound species}]$ ($\text{p}K'_a$ values of three Zn^{2+} -bound waters in **1**·(H_2O)₃ are 6.08, 7.25, and 8.63, respectively)^[8] and apparent affinity constants $K_{\text{app}} = [\mathbf{6}]/[\mathbf{1}]^4[\text{TCA}]^4$ (M^{-7}) were determined by means of the program BEST.^[28] All the sigma fit values defined in the program are smaller than 0.05. The $K_w = a_{\text{H}^+} \cdot a_{\text{OH}^-}$, $K'_w = [\text{H}^+][\text{OH}^-]$, and f_{H^+} values used at 25°C were $10^{-14.00}$, $10^{-13.79}$, and 0.825, respectively. The corresponding mixed constants, $K_2 = [\text{HO}^- \text{-bound species}]a_{\text{H}^+}/[\text{H}_2\text{O-bound species}]$, were derived from $[\text{H}^+] = a_{\text{H}^+}/f_{\text{H}^+}$. The species distribution values (%) against $\text{pH} = (-\log[\text{H}^+] + 0.084)$ were obtained using the program SPE.^[28]

Partition experiments of organic guest molecules: A 1:1 (v/v) mixture of an organic guest molecule (2.0 mm) in D_2O at pD 7.0 and 1-octanol (saturated with D_2O in advance) was vigorously stirred at room temperature for 30 min. The resulting solution was centrifuged (3000 rpm for 20 min), and an aliquot of the D_2O phase was removed, to which a determined amount of a solution of a reference compound (benzene sulfonate and/or TSP) in D_2O was added. The concentration of the guest molecule in D_2O was calculated with respect to the concentration of reference compounds (benzene sulfonate and/or TSP).

Acknowledgement

E.K. and S.A. are thankful for Ministry of Education and Science for Grant-in-Aid (No. 08249103, No. 12470479, No. 12033237, No. 12771355, and No. 13557195). S.A. is thankful for the Research Foundation for Pharmaceutical Sciences, Japan and the Asahi Glass Foundation, Japan. We are thankful for Prof. Makoto Fujita (Nagoya University) for providing us with the $[\text{Pd}_6\text{L}_2]_4$ complex **9** and for Ms. Sanae Furusho (JASCO International) for ESI-MS experiments. We are grateful for being allowed the use of the NMR instrument (a JEOL Alpha 400 MHz spectrometer) in the Research Center for Molecular Medicine (RCMM) in Hiroshima University.

- [1] a) J.-M. Lehn, *Supramolecular Chemistry: Concepts and Perspectives*, VCH, Weinheim, **1995**; b) H.-J. Schneider, A. Yatsimirsky, *Principles and Methods in Supramolecular Chemistry*, Wiley, Chichester, **2000**; c) G. M. Whitesides, J. P. Mathias, C. T. Seto, *Acc. Chem. Res.* **1995**, *28*, 37–44; d) D. Philip, J. F. Stoddart, *Angew. Chem.* **1996**, *108*, 1242–1286; *Angew. Chem. Int. Ed. Engl.* **1996**, *35*, 1155–1196; e) C. Piguet, G. Bernardinelli, G. Hopfgartner, *Chem. Rev.* **1997**, *97*, 2005–2062; f) B. J. Holliday, C. A. Mirkin, *Angew. Chem.* **2001**, *113*, 2076–2097; *Angew. Chem. Int. Ed.* **2001**, *40*, 2022–2043; g) L. J. Prins, D. N. Reinhoudt, P. Timmerman, *Angew. Chem.* **2001**, *113*, 2446–2492; *Angew. Chem. Int. Ed.* **2001**, *40*, 2382–2426.
- [2] a) M. Fujita, *Molecular Self-Assembly Organic Versus Inorganic Approaches*, Springer, Berlin, **2000**; b) M. Fujita, *Chem. Soc. Rev.* **1998**, *27*, 417–425; c) M. Fujita, K. Umemoto, M. Yoshizawa, N. Fujita, T. Kusukawa, K. Biradha, *Chem. Commun.* **2001**, 509–518.
- [3] a) B. Olenyuk, J. A. Whiteford, A. Fechtenkötter, P. J. Stang, *Nature* **1999**, *398*, 796–799; b) B. Olenyuk, A. Fechtenkötter, P. J. Stang, *J. Chem. Soc. Dalton Trans.* **1998**, 1707–1728; c) S. Leininger, B. Olenyuk, P. J. Stang, *Chem. Rev.* **2000**, *100*, 853–908; d) A. Ikeda, K. Sonoda, S. Shinkai, *Chem. Lett.* **2000**, 1220–1221; e) Z. Zhong, A. Ikeda, S. Shinkai, S. Sakamoto, M. Yamaguchi, *Org. Lett.* **2001**, *3*, 1085–1087; f) N. Cuminetti, M. H. K. Ebbing, P. Prados, J. de Mendoza, E. Dalcaneale, *Tetrahedron Lett.* **2001**, *42*, 527–530; g) O. D. Fox, N. K. Dalley, R. G. Harrison, *J. Am. Chem. Soc.* **1998**, *120*, 7111–7112; h) N. Fatin-Rouge, S. Blanc, A. Pfeil, A. Rigault, A.-M. Albrecht-Gary, J.-M. Lehn, *Helv. Chim. Acta* **2001**, *84*, 1694–1711.
- [4] a) D. L. Caulder, K. N. Raymond, *J. Chem. Soc. Dalton Trans.* **1999**, 1185–1199; b) D. L. Caulder, K. N. Raymond, *Acc. Chem. Rev.* **1999**, *32*, 975–982; c) J. Xu, T. N. Parac, K. N. Raymond, *Angew. Chem.* **1999**, *111*, 3055–3058; *Angew. Chem. Int. Ed.* **1999**, *38*, 2878–2882; d) D. W. Johnson, J. Xu, R. W. Saalfrank, K. N. Raymond, *Angew. Chem.* **1999**, *111*, 3058–3061; *Angew. Chem. Int. Ed.* **1999**, *38*, 2882–2885.

- [5] For review: a) E. Kimura, *Tetrahedron* **1992**, *48*, 6175–6217; b) E. Kimura, *Prog. Inorg. Chem.* **1994**, *41*, 443–491; c) E. Kimura, M. Shionoya, *Met. Ions Biol. Syst.* **1996**, *33*, 29–52; d) E. Kimura, T. Koike, M. Shionoya, *Struct. Bonding*, **1997**, *89*, 1–28; e) E. Kimura, T. Koike, *Chem. Commun.* **1998**, 1495–1500; f) E. Kimura, T. Koike in *Bioinorganic Catalysis* (Eds: J. Reedijk, E. Bouwman), Marcel Dekker, New York, **1999**, pp. 33–54; g) E. Kimura, E. Kikuta, *J. Biol. Inorg. Chem.* **2000**, *5*, 139–155; h) E. Kimura, *Acc. Chem. Res.* **2001**, *34*, 171–179.
- [6] a) E. Kimura, T. Ikeda, M. Shionoya, *Angew. Chem.* **1995**, *107*, 711–712; *Angew. Chem. Int. Ed. Engl.* **1995**, *34*, 663–664; b) H. Fujioka, T. Koike, N. Yamada, E. Kimura, *Heterocycles* **1996**, *42*, 775–787; c) T. Koike, M. Takashige, E. Kimura, H. Fujioka, M. Shiro, *Chem. Eur. J.* **1996**, *2*, 617–623; d) E. Kimura, H. Kitamura, K. Ohtani, T. Koike, *J. Am. Chem. Soc.* **2000**, *122*, 4668–4677.
- [7] S. Aoki, M. Shiro, T. Koike, E. Kimura, *J. Am. Chem. Soc.* **2000**, *122*, 576–584, and references therein.
- [8] E. Kimura, S. Aoki, T. Koike, M. Shiro, *J. Am. Chem. Soc.* **1997**, *119*, 3068–3076.
- [9] a) R. C. Hirt, R. G. Schmitt, H. L. Strauss, J. G. Koren, *J. Chem. Eng. Data* **1961**, *6*, 610–613; b) A. E. Beezer, J. C. Chudy, *Thermochim. Acta* **1973**, *6*, 231–237; c) F. Belaj, R. Tripolt, E. Nachbauer, *Monatsh. Chem.* **1990**, *121*, 99–108; d) K. R. Henke, J. C., Bryan, M. P. Elless, *Powder Diffraction* **1997**, *12*, 7–12; e) K. R. Henke, D. A. Atwood, *Inorg. Chem.* **1998**, *37*, 224–227.
- [10] a) B. Krebs, G. Henkel, *Angew. Chem.* **1991**, *103*, 785–804; *Angew. Chem. Int. Ed. Engl.* **1991**, *30*, 769–788; b) T. Koike, M. Takamura, E. Kimura, *J. Am. Chem. Soc.* **1994**, *116*, 8443–8449; c) O. D. Fox, M. G. B. Drew, P. D. Beer, *Angew. Chem.* **2000**, *112*, 139–144; *Angew. Chem. Int. Ed.* **2000**, *39*, 135–140.
- [11] For reviews on (supra)molecular capsules, see: a) D. J. Cram, J. M. Cram, *Container Molecules and Their Guests* (Ed.: J. F. Stoddart), Royal Society of Chemistry, Cambridge, **1994**; b) M. M. Conn, J. Rebek, Jr., *Chem. Rev.* **1997**, *97*, 1647–1668; c) B. Linton, A. D. Hamilton, *Chem. Rev.* **1997**, *97*, 1669–1680; d) C. J. Jones, *Chem. Soc. Rev.* **1998**, *27*, 289–299; e) A. Jasat, J. C. Sherman, *Chem. Rev.* **1999**, *99*, 931–967.
- [12] a) L. R. MacGillivray, J. L. Atwood, *Angew. Chem.* **1996**, *111*, 1080–1096; *Angew. Chem. Int. Ed.* **1999**, *38*, 1018–1033; b) P. Donzalez-Duarte, W. Clegg, I. Casals, J. Sola, J. Rius, *J. Am. Chem. Soc.* **1998**, *120*, 1260–1266; c) G. F. Swiegers, T. J. Malefetse, *Chem. Rev.* **2000**, *100*, 3483–3537.
- [13] Four nitrate anions and four water molecules were found in the inner cavity **8**.
- [14] For previous guest-induced organization of self-assembly: a) M. Fujita, S. Nagao, K. Ogura *J. Am. Chem. Soc.* **1995**, *117*, 1649–1650; b) M. Fujita, O. Sasaki, T. Mitsuhashi, T. Fujita, J. Yazaki, K. Yamaguchi, K. Ogura, *Chem. Commun.* **1996**, 1535–1536. c) T. Martin, U. Obst, J. Rebek, Jr., *Science* **1998**, *281*, 1842–1845; d) T. Martin, U. Obst, J. Rebek, Jr., *Science* **1998**, *281*, 1842–1845; e) S. B. Lee, S. Hwang, D. S. Chung, H. Yun, J.-I. Hong, *Tetrahedron Lett.* **1998**, *39*, 873–876; f) M. Scherer, D. L. Caulder, D. W. Johnson, K. N. Raymond, *Angew. Chem.* **1999**, *111*, 1690–1694; *Angew. Chem. Int. Ed.* **1999**, *38*, 1588–1592; g) K. Umamoto, K. Yamaguchi, M. Fujita, *J. Am. Chem. Soc.* **2000**, *122*, 7150–7151; h) S. Saito, C. Nuckolls, J. Rebek, Jr., *J. Am. Chem. Soc.* **2000**, *122*, 9628–9630.
- [15] For examples of kinetically inert Zn^{II}-cyclen guest complexes: a) S. Aoki, C. Sugimura, E. Kimura, *J. Am. Chem. Soc.* **1998**, *120*, 10094–10102; b) E. Kimura, M. Kikuchi, H. Kitamura, T. Koike, *Chem. Eur. J.* **1999**, *5*, 3113–3123; c) S. Aoki, E. Kimura, *J. Am. Chem. Soc.* **2000**, *122*, 4542–4548; d) E. Kimura, E. Kikuta, *Prog. React. Kinet. Mech.* **2000**, *25*, 1–64.
- [16] By addition of 10% (v/v) CD₃CN or 10% (v/v) [D₆]DMSO to the **6**-TSP complex in D₂O at pD 7.0, proton peaks corresponding TSP in **6** disappeared and another single species of **6** appeared, possibly corresponding to CD₃CN/[D₆]DMSO-encapsulated **6** as a result of displacement of TSP by CD₃CN or [D₆]DMSO. The ¹H and ¹³C NMR spectra of **6** were taken in CD₃CN/D₂O (10/90). We could not determine how many molecules of CD₃CN or [D₆]DMSO were encapsulated in **6**. The addition of 10% (v/v) CD₃OD to a solution of **6** caused negligible change.
- [17] Our preliminary results of stopped-flow experiments suggest that the 4:4 complexation of **1** and TCA occurs in millisecond order in the presence of TPA at pH 7.0 and 25°C. The details will be described elsewhere.
- [18] W. Oppolzer, C. Chapuis, G. Bernardinelli, *Helv. Chim. Acta* **1984**, *67*, 1397–1401.
- [19] The length of congressane is about 8.5 Å by molecular model study, which barely fits in the inner cavity **8**.
- [20] The guest encapsulation in the supramolecular complex **6** has been concluded also from the UV titration (and competitive UV titration) and X-ray structure analysis. Very little upfield shifts (0–0.1 ppm) were observed in ¹H NMR spectra by the interaction of guest compounds with **1** or TCA alone.
- [21] The ¹H NMR spectra (aromatic regions) of several typical **6**-guest complexes are shown in the Supporting Information. The aromatic peaks of **6**/ammonium cation complexes such as **6**-TEA and **6**-TPA appear with downfield shift at $\delta = 7.42$ and 7.53, respectively, probably because of deshielding effect by the encapsulated ammonium cations. For comparison, the aromatic peaks of encapsulation complexes such as **6**-TSP, **6**-ADM, **6**-nitrophenol, and **6**-CST appeared at $\delta = 7.0$ –7.2. Aromatic protons of **6** in most of the **6**-guest complexes were symmetric in the ¹H NMR spectra. We presume that a guest molecule tends to rotate freely in the inner cavity at room temperature.
- [22] A. I. Sobolevsky, S. G. Koshelev, B. I. Khodoro, *Biol. Membr.* **1999**, *16*, 64–71.
- [23] We could not see a correlation between log *K*_{enc} values and partition yields to 1-octanol of guest molecules (Table 1).
- [24] The relatively large *R* values and low reflection/variable ratio of **6** and **6**-ADM complexes were due to relatively poor quality of the crystals and small $2\theta_{\max}$ values (45.0 or 40.0°). Although these *R* values were as far as we could go down, the supramolecular frameworks are definitely convincing from these X-ray crystal structure analysis and other experimental data discussed in the following sections. Use of Cu radiation for the X-ray crystal structure analysis of these two crystals did not improve the results.
- [25] The aromatic carbon peaks of TCA³⁻ (at pD 13.5) appeared at $\delta = 184.81$ and those of TCA units in **6**-ADM complex (at pD 7.0) at $\delta = 182.75$ in the ¹³C NMR spectra in D₂O at pD 7.0, which supported a conclusion that all the three protons of TCA units in **6**-ADM complex are deprotonated in neutral aqueous solution.
- [26] Interestingly, ADM came out from the **6**-ADM complex upon the addition of a large excess of CD₃CN or [D₆]DMSO (up to 10% (v/v)) forming the **6**-CD₃CN (or [D₆]DMSO) complex as described in ref. [16].
- [27] TPA stabilizes the cage as a guest, but has negligible effect on pH of solution. It was confirmed that **6** (0.25 mM) quantitatively encapsulated TPA at [I] = [TCA] = [TPA] = 1.0 mM by ¹H NMR spectroscopy in D₂O at pD 7.0 and 8.0.
- [28] A. E. Martell, R. J. Motekaitis, *Determination and Use of Stability Constants*, 2nd ed., VCH, New York, **1992**.
- [29] In ¹H NMR experiments, proton signals of HEPES showed negligible upfield shifts in the presence of **6**, implying that HEPES was not a guest.
- [30] It should be noted that [6] in Equation (7) includes the concentrations of other 1:1 (= *n*:*n*) **1**:TCA³⁻ species equilibrating with **6** in aqueous solution.
- [31] The ¹H NMR of **6** (1.0 mM) in the presence of 2,4-DNP (1.0 mM) and ADCA (1.0 mM) in D₂O at pD 7.0 indicated an almost equal amount of encapsulated 2,4-DNP and ADCA. This fact supports that 2,4-DNP and ADCA have almost the same encapsulation constants.
- [32] a) C. Reichardt, *Solvent and Solvent Effects in Organic Chemistry*, VCH, Weinheim, **1988**; b) Y. Marcus, *The Properties of Solvents*, Wiley, Chichester, **1998**; c) B. B. Raju, S. M. B. Costa, *Phys. Chem. Chem. Phys.* **1999**, *1*, 3539–3547; d) B. B. Raju, S. M. B. Costa, *J. Phys. Chem. B* **1999**, *103*, 4309–4317.
- [33] We do not exclude the possibility that the hydrophobicity in the inner cavity **8** is underestimated due to the equilibrium between the free and encapsulated DEACC.
- [34] Although there have been numerous numbers of highly functionalized derivatives of cyclodextrins (*Comprehensive Supramolecular Chemistry*, Vol. 3 (Eds.: J. L. Atwood, J. E. D. Davies, D. D. MacNicol, F.

- Vögtle), Pergamon, Oxford, **1996**), we have just compared our system with commercially available α - and β -cyclodextrins in this study.
- [35] M. Fujita, D. Oguro, M. Miyazawa, H. Oka, K. Yamaguchi, K. Ogura, *Nature* **1995**, *378*, 469–471.
- [36] a) F. Cramer, W. Saenger, H.-C. Spatz, *J. Am. Chem. Soc.* **1967**, *89*, 14–20; b) Y. Kanda, Y. Yamamoto, Y. Inoue, R. Chujo, S. Kobayashi, *Bull. Chem. Soc. Jpn.* **1989**, *62*, 2002–2008; c) Connors, K. A. *Chem. Rev.* **1997**, *97*, 1325–2357.
- [37] M. Komiyama, M. L. Bender, *J. Am. Chem. Soc.* **1978**, *100*, 2259–2260.
- [38] Negligible interaction between α -, or β -CD (1 mM) and TCA was observed in the ^1H NMR titrations in aqueous solution at pD 7.0.
- [39] From this value, $\log K_{\text{enc}}$ for the **6**-ADCA complex was calculated to be 5.1, which showed a fairly good agreement with the $\log K_{\text{enc}}$ value 5.5 ± 0.3 determined by competitive UV titration experiments described above.
- [40] a) J. C. Harrison, M. R. Eftink, *Biopolymers* **1982**, *21*, 1153–1166. b) T. Kuwabata, A. Nakamura, A. Ueno, Fujio Toda, *J. Phys. Chem.* **1994**, *98*, 6297–6303.
- [41] For comparison, the $\text{p}K_{\text{a}}$ value of propionic acid is 6.88 in 70:30 1,4-dioxane/ H_2O , while it is 4.83 in 10:90 1,4-dioxane/ H_2O (E. Casassa, G. Fonrodona, A. de Juan, *Inorg. Chim. Acta* **1991**, *187*, 187–195).
- [42] E. Eliel, S. H. Wilen, L. N. Mander, *Stereochemistry of Organic Compounds*, Wiley, New York, **1994**.
- [43] For examples of supramolecular chirality transfer: a) R. K. Castellano, C. Nuckolls, J. Rebek, Jr., *J. Am. Chem. Soc.* **1999**, *121*, 11156–11163; b) A. Sugasaki, M. Ikeda, M. Takeuchi, A. Robertson, S. Shinkai, *J. Chem. Soc. Perkin Trans. 1*, **1999**, 3259–3262; c) L. J. Prins, J. Huskens, F. deJong, P. Timmerman, D. N. Reinhoudt, *Nature*, **1999**, *398*, 498–502; d) E. Yashima, K. Maeda, Y. Okamoto, *Nature*, **1999**, *399*, 449–451; e) Y. Mitzuno, T. Aida, K. Yamaguchi, *J. Am. Chem. Soc.* **2000**, *122*, 5278–5285; f) H. Nakashima, J. R. Koe, K. Torimitsu, M. Fujiki, *J. Am. Chem. Soc.* **2001**, *123*, 4847–4848. g) A. J. Terpin, M. Ziegler, D. W. Johnson, K. N. Raymond, *Angew. Chem.* **2001**, *113*, 161–164; *Angew. Chem. Int. Ed.* **2001**, *140*, 157–160.
- [44] To determine enantiomeric excess of the (1*S*,2*R*,4*R*)-(–)-CST-encapsulating **6**, we observed its ^1H NMR spectra (1 mM) in the presence of (1*S*)-CSA (1 mM, an anionic non-guest) in D_2O . However, diastereomeric proton peaks were not observed.
- [45] We also isolated the **6**-(3-NP) (colorless prisms), **6**-(4-NP) $^-$ (yellow prisms), **6**-(2,4-DNP) $^-$ (yellow prisms), and **6**-((1*S*,2*R*,4*R*)-(–)-CST) (colorless prisms) complexes and carried out electrospray mass spectrometry (ESI-MS) experiments (+ mode) of these complexes. Among them, the 3+, 4+, 5+, 6+, and 7+ species with mass-to-charge ratios (m/z) were observed for **6**-(3-NP) and **6**-((1*S*,2*R*,4*R*)-(–)-CST) complexes (see the Supporting Information).

Received: September 17, 2001 [F3558]